

Using Stochastically Generated Subcolumns to Represent Cloud Structure in a Large-Scale Model

ROBERT PINCUS

CIRES/Climate Diagnostics Center, and NOAA/Earth System Research Laboratory, Boulder, Colorado

RICHARD HEMLER

NOAA/Geophysical Fluid Dynamics Laboratory, Princeton, New Jersey

STEPHEN A. KLEIN

Atmospheric Sciences Division, Lawrence Livermore National Laboratory, Livermore, California

(Manuscript received 9 December 2005, in final form 27 February 2006)

ABSTRACT

A new method for representing subgrid-scale cloud structure in which each model column is decomposed into a set of subcolumns has been introduced into the Geophysical Fluid Dynamics Laboratory's global atmospheric model AM2. Each subcolumn in the decomposition is homogeneous, but the ensemble reproduces the initial profiles of cloud properties including cloud fraction, internal variability (if any) in cloud condensate, and arbitrary overlap assumptions that describe vertical correlations. These subcolumns are used in radiation and diagnostic calculations and have allowed the introduction of more realistic overlap assumptions. This paper describes the impact of these new methods for representing cloud structure in instantaneous calculations and long-term integrations. Shortwave radiation computed using subcolumns and the random overlap assumption differs in the global annual average by more than 4 W m^{-2} from the operational radiation scheme in instantaneous calculations; much of this difference is counteracted by a change in the overlap assumption to one in which overlap varies continuously with the separation distance between layers. Internal variability in cloud condensate, diagnosed from the mean condensate amount and cloud fraction, has about the same effect on radiative fluxes as does the ad hoc tuning accounting for this effect in the operational radiation scheme. Long simulations with the new model configuration show little difference from the operational model configuration, while statistical tests indicate that the model does not respond systematically to the sampling noise introduced by the approximate radiative transfer techniques introduced to work with the subcolumns.

1. Cloud vertical structure in the global atmospheric model AM2

Current global models of the atmosphere, such as those used to predict short-term weather or long-term climate change, have horizontal grid spacings of tens to hundreds of kilometers. At these resolutions, many processes, including the treatment of clouds and radiation, must be treated statistically. In particular, calcu-

lations of radiation and precipitation fluxes require a conceptual model of subgrid-scale cloud structure. This model usually accounts for the possibility of horizontal variations within each grid cell: some parts of the grid may be cloudy and others clear, for example, and some parts of the cloud may be thicker than others. The conceptual model also describes the relationship between the subgrid-scale structures in different vertical layers.

In the global atmospheric model developed by the Geophysical Fluid Dynamics Laboratory (AM2; GFDL Global Atmospheric Model Development Team 2004), cloud structure is relatively simple. Within each grid cell, the model predicts the areal fraction occupied by clouds and the grid-mean mass concentrations of cloud ice and liquid and uses the random overlap assumption

Corresponding author address: Dr. Robert Pincus, CIRES/Climate Diagnostics Center, 325 Broadway, R/CDC1, Boulder, CO 80305.

E-mail: robert.pincus@colorado.edu

to determine structure in the vertical. Clouds are assumed to be uniform within the cloudy portion of each cell. The overlap assumption is implemented in radiation calculations by computing the transmittance (and reflectance, in the shortwave) of each layer in the column as the cloud fraction-weighted sum of clear- and cloudy-sky transmittance. Fluxes of stratiform precipitation are computed separately for the clear and cloudy portions of each layer beginning at the top of the model atmosphere and using the fractional areas occupied by cloud-over-cloud, cloud-over-clear, etc. transitions at each layer interface (Jakob and Klein 2000).

We had several reasons to want to change this state of affairs. One was the reliance on the random overlap assumption, which is inconsistent with observations (Hogan and Illingworth 2003; Mace and Benson-Troth 2002; Tian and Curry 1989) and produces vertically projected cloud fractions that depend on the number of model layers spanning a given cloud layer. The implementation in AM2 was also inflexible, because neither the random overlap assumption nor the assumption of cloud homogeneity within the model grid cell could be relaxed. The small- (subgrid-) scale variability in cloud condensate that exists in nature was treated in AM2 by tuning parameters in physical parameterizations. In radiation calculations, for example, cloud ice and liquid water concentrations are reduced by 15% before computing radiative properties (Tiedtke 1996). We are considering a cloud scheme that takes a more physically based approach to subgrid-scale variability by assuming a probability distribution function (PDF) for the total water specific humidity within each grid cell (Tompkins 2002). We hope that this approach will reduce or eliminate the need for tuning, but it is not clear how we would couple the potentially complicated distributions of condensate predicted by the assumed PDF cloud scheme to existing methods for computing radiation and precipitation fluxes.

This paper describes the implementation in AM2 of a general scheme to represent subgrid-scale cloud structure, including cloud overlap, as a set of subcolumns within each grid column. We detail the ways subcolumns are generated in AM2 and how these subcolumns are linked to radiation and precipitation calculations and to model diagnostics. We then take advantage of the flexible way cloud structure can be represented using subcolumns to calculate the impact that overlap and subgrid-scale homogeneity assumptions have on the radiative fluxes computed from the cloud fields produced by AM2. The impact on multiyear interactive simulations with specified sea surface temperature is then assessed.

2. Representing cloud structure using an ensemble of subcolumns

a. Creating ensembles of subcolumns

We represent cloud structure within each column of the large-scale model as an ensemble of stochastically generated subcolumns (Räisänen et al. 2004). Each layer within each subcolumn is homogeneous, with a cloud fraction of either zero or one and uniform cloud liquid and ice concentration. The ensemble as a whole, however, reproduces the probability distribution function of cloud ice and liquid, including the cloud fraction, within each layer, and also obeys the overlap assumptions that specify the correlation of clouds and possibly water vapor in the vertical. Arbitrarily complicated PDFs and overlap assumptions can be represented, and sampling errors for cloud properties (i.e., cloud fraction or the cloud condensate PDF) within individual model columns can be controlled by varying the number of subcolumns used. The columns are constructed by drawing random samples from the distribution of condensate (including the clear sky) while simultaneously imposing vertical structure. Detailed discussion of how ensembles of subcolumns are generated may be found in Räisänen et al. (2004) and Pincus et al. (2005). An example of one set of subcolumns produced from a profile of cloud properties is shown in Fig. 1.

We include four possible overlap assumptions: random, maximum, maximum random, and one in which overlap changes inverse exponentially from maximum to random as the distance between a pair of layers increases (Bergman and Rasch 2002; Hogan and Illingworth 2000). The latter assumption, which we call “exponentially decaying overlap,” requires the specification of a length scale but has the advantage that the vertically projected cloud fraction in a given column does not depend on the number of layers over which a cloud extends. We also include an option to diagnose the subgrid-scale distribution of condensate within each grid cell in a way that is consistent with both the model’s current predictions of cloud fraction and mean condensate and with the PDF used in the cloud scheme that we are developing. The method for estimating variability is detailed in the appendix. When internal variability is included, the overlap of cloud existence and condensate concentration is specified by defining the overlap assumption in terms of the rank correlation of total water (Pincus et al. 2005).

The subcolumns are created using a pseudorandom number generator. In our experience, incorporating a random number generator into a deterministic forecast model requires the careful balancing of two concerns.

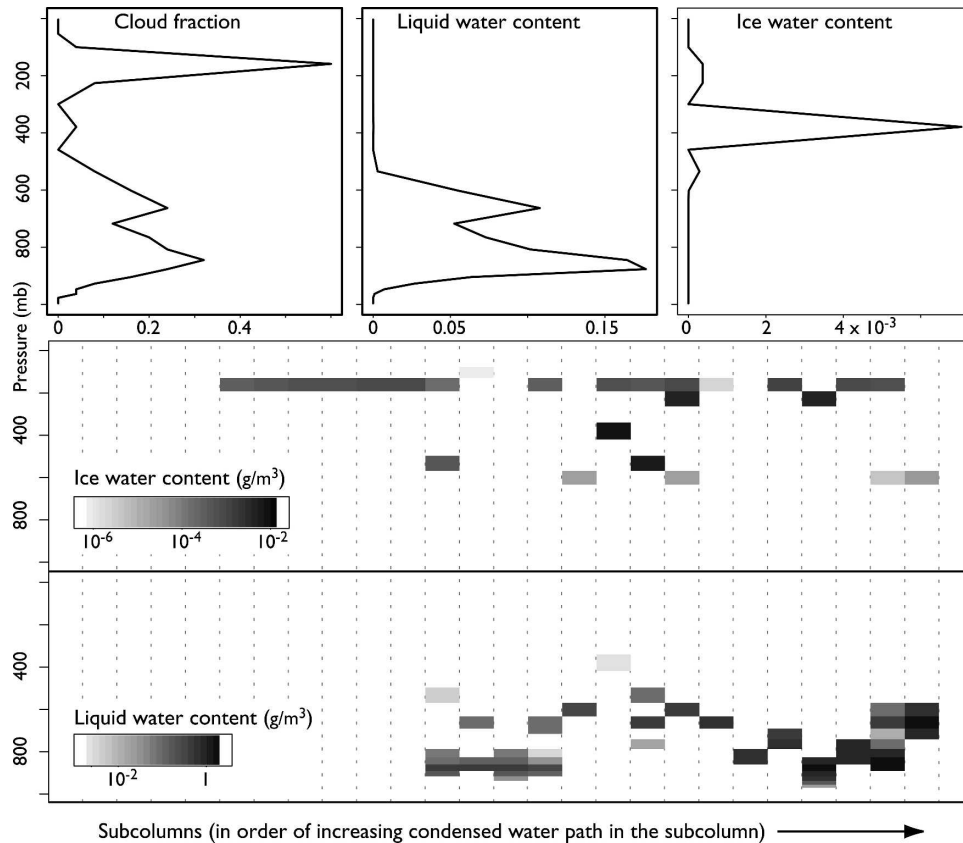


FIG. 1. Example subcolumns created from model profiles of cloud fraction and liquid and ice water concentrations. (top) Profiles of cloud fraction and liquid and ice water concentrations taken from a single column of AM2 at a single time step. (middle), (bottom) Twenty-five subcolumns created stochastically using an exponentially decaying overlap assumption with a scale length of 1 km and internal variability in cloud water and ice concentrations diagnosed from the cloud fraction and mean condensate amount. Gray shades indicate ice and liquid water concentrations. The columns are generated in random order but are shown here in order of ascending ice-plus-liquid water paths.

On the one hand, model forecasts should be completely reproducible and depend only on the state of the atmosphere. In particular, forecasts may not depend on the number of processors on which the model is run or on how long the model has been running. In our implementation, this is enforced by using a separate random number stream for each large-scale model grid column and initializing each sequence uniquely and deterministically at the beginning of each time step. On the other hand, techniques that rely on Monte Carlo sampling (like the decomposition of columns into subcolumns) require samples, and hence random number sequences, that are uncorrelated in space and time. Unfortunately, some popular random number generators (e.g., RAN0 and RAN1 from Press et al. 1986), given similar seeds, produce sequences whose first few values are correlated. After extensive experimentation, we chose a FORTRAN 90 implementation of the Mersenne Twister (Matsumoto and Nishimura 1998) initialized with a

vector of integers comprising the model date and time and the latitude and longitude of the column center.

b. Computing process rates using subcolumns

Once a given model grid column has been divided into subcolumns, all-sky radiation fluxes and heating rates within the column may be computed using the independent column approximation (ICA), that is, by calculating the broadband flux in each subcolumn and averaging. Each of these radiation calculations requires integrating across the spectrum, typically by computing fluxes in some number of spectral intervals and composing a weighted average. Given J subcolumns s_j and K spectral intervals centered on wavelengths λ_k with spectral weights $w(\lambda_k)$, the column-mean ICA flux $\langle F^{ICA} \rangle$ is defined as

$$\langle F^{ICA} \rangle = \frac{1}{J} \sum_j F(s_j) = \frac{1}{J} \sum_j \sum_k w(\lambda_k) F_\lambda(s_j, \lambda_k). \quad (1)$$

Radiative fluxes are computed every 3 h in AM2, as compared with the 0.5 h time step for other physical parameterizations, and yet radiation consumes about 30% of the model runtime. To avoid the large expense that would be incurred by implementing (1) directly, we use a simple all-sky implementation of the Monte Carlo ICA (McICA; Pincus et al. 2003). The radiation scheme used in AM2 has 18 spectral intervals in the shortwave and 7 in the longwave. We generate a random sample of $18 + 7 = 25$ subcolumns in each model grid column. Radiative transfer in each spectral band is computed on a different subcolumn and the column-mean all-sky radiative fluxes and heating rates are determined by summing across the spectral intervals (equivalently, the subcolumns), that is,

$$\langle F^{ICA} \rangle \approx \sum_k^K w(\lambda_k) F(s_k, \lambda_k). \quad (2)$$

Generating the subcolumns and implementing (2) increases the runtime of AM2 by 2%–3%.

Compared with other radiative transfer schemes (e.g., Mlawer et al. 1997; Räisänen et al. 2005), AM2 uses relatively few spectral intervals, so we have been able to include the option to use the ICA by applying (1) directly. The model runs about 3 times slower using ICA than McICA though, so this is not a viable alternative for routine integrations.

Calculations of stratiform precipitation could, in principle, be treated using ICA, but this would be very expensive because no time-saving algorithm like McICA has yet emerged (though see Larson et al. 2005 for a promising candidate). In our implementation of AM2, subgrid-scale inhomogeneity in condensate amounts is neglected in precipitation calculations, and we approximate the influence of the overlap assumption by determining the likelihood of transitions between clear and cloudy skies (Jakob and Klein 2000). This means that the overlap assumption affects both radiation and precipitation calculations, while assumptions about in-cloud inhomogeneity affect only the radiative fluxes.

c. Computing model diagnostics using subcolumns

The use of subcolumns to represent subgrid-scale structure in large-scale models has a historical precedent: the technique has been in use for more than a decade as part of the International Satellite Cloud Climatology Project (ISCCP) simulator (Klein and Jakob 1999; Webb et al. 2001; Yu et al. 1996). The ISCCP (Rossow and Schiffer 1999) produces joint histograms of cloud-top pressure and cloud optical thickness as a function of location. These histograms provide a more

refined dataset for model evaluation than do top-of-atmosphere (TOA) radiative fluxes but cannot be compared directly with large-scale model profiles of cloud fraction and condensate. The ISCCP simulator bridges this gap by creating an ensemble of columns, roughly mimicking the ISCCP retrieval process on each subcolumn, and aggregating the results.

The ISCCP simulator consists of two parts: one generates subgrid-scale structure according to overlap rules (assuming no in-cloud variability) and the other simulates retrievals made in those subcolumns. We recoded the simulator to separate these functions. We also added an option to produce the parameter $\varepsilon = 1 - \hat{\tau}/\bar{\tau}$ (Rossow et al. 2002), where $\bar{\tau}$ is the (linear) mean optical depth of the cloudy subcolumns and $\hat{\tau}$ is the radiative-mean optical thickness, that is, the optical thickness that produces the mean albedo of the cloudy subcolumns. The quantity ε describes the variability of optical depth τ within each grid column. It is equal to 0 when optical depth is uniform in the column and grows as the variability increases. In AM2, retrieval simulations now use the subcolumns generated for radiation calculations so that the ISCCP diagnostics reported by the model are consistent with the cloud structure used in the process rate calculations.

3. How radiative fluxes depend on cloud structure assumptions and implementation details

In this section, we use the flexibility of stochastically generated subcolumns to assess the impact of assumptions regarding overlap and subgrid-scale inhomogeneity on the instantaneous radiation and precipitation fluxes in AM2. These impacts depend on the profiles of cloud fraction and cloud condensate produced by the model, so results from other models (e.g., Morcrette and Jakob 2000) provide only loose guidance. To sample the diurnal and seasonal cycles of cloud properties, we select profiles produced by AM2 on a $2^\circ \times 2.5^\circ$ latitude–longitude grid every 3 h beginning at 0000 UTC on the first day of every month for 1 yr (1983), taken from a run in which sea surface temperatures are specified. Results below are the average of these 96 time steps and, in most cases, a global average weighted by the area of each model grid column. The same profiles of cloud properties are used in all radiation calculations in this section (i.e., the calculations are diagnostic).

Figure 2 shows the mean difference between TOA radiative fluxes as computed (i) using the standard implementation of overlap and (ii) using the stochastic subcolumns to represent random overlap of uniform

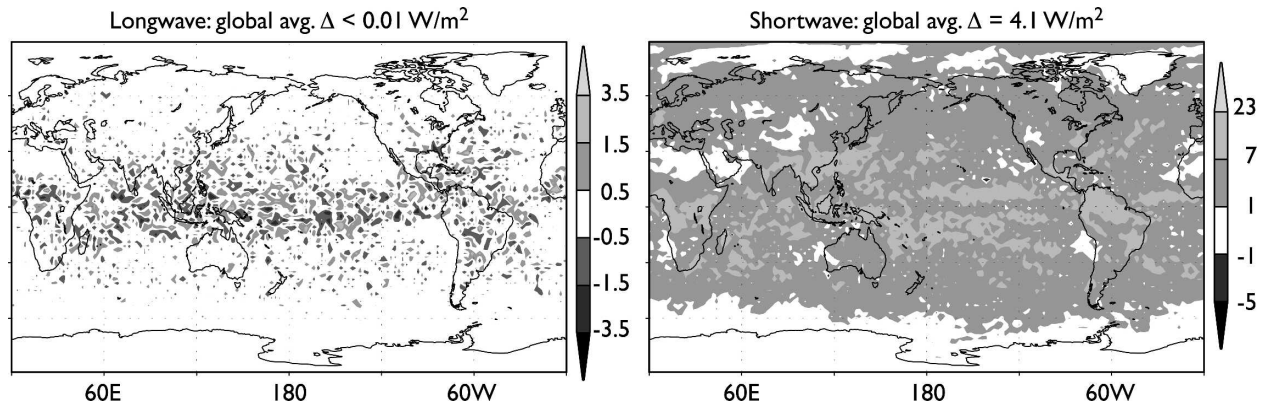


FIG. 2. The difference in TOA radiative fluxes due to two treatments of cloud overlap. The operational version of AM2 implements random overlap by averaging clear- and cloudy-sky reflectance and transmittance according to cloud fraction and then computing radiative transfer in a single column. An alternative is to construct an ensemble of subcolumns (as described in the text), compute radiative transfer in each subcolumn, and average the results (ICA). This figure shows the difference between these two calculations (ICA minus the original implementation) using the same cloud fields. (left) Longwave fluxes show some sampling noise from the subcolumn generation, but this noise is spatially uncorrelated and has a global mean difference of less than 0.01 W m^{-2} . (right) Reflected shortwave fluxes, however, are greater in almost all locations when ICA is used, and the subcolumns reflect more sunlight by about 4.1 W m^{-2} in the global mean.

clouds. The difference in the two calculations of longwave fluxes (left panel) is spatially uncorrelated and almost exactly 0, while the difference between the shortwave flux calculations (right panel) has substantial spatial autocorrelation. Furthermore, the global mean reflected flux computed using subcolumns is 4.1 W m^{-2} larger than the operational implementation. (The calculations in this section include all columns, including those with no clouds or those with no incoming solar radiation, because it is the global average bias that affects model evolution.) The bias in reflected solar radiation between the two implementations of the same overlap, though discouraging, is not surprising. Bulk treatments of overlap (i.e., treating the transmittance of the layer as a weight sum of clear- and cloudy-sky transmittance) are known to disagree in general with column-by-column radiative transfer calculations, especially in the shortwave where multiple scattering is common (Barker et al. 2003). The difference increases as the overlap assumption becomes more important in determining radiative fluxes, that is, as the number of

partially cloudy layers increases (as in regions of deep convection like the Tropics). In large samples, the difference does not depend on whether ICA or McICA is used to compute the radiative fluxes in the subcolumns.

One advantage of using subcolumns is that it becomes relatively easy to test the impact of particular assumptions about cloud structure (Pincus et al. 2003). Table 1, for example, shows the change in globally averaged TOA fluxes and vertically projected cloud fraction as the overlap assumption applied to AM2's cloud fields is changed and clouds are assumed to be uniform, while Table 2 shows the impact of introducing diagnostic in-cloud inhomogeneity while the overlap assumption is fixed. Table 2 indicates that diagnostic inhomogeneity (based on the model's cloud fraction and mean condensate amount and on two assumptions about the shape of the distribution of total water) has about the same effect on TOA fluxes as does the tuning of cloud optical properties (based on a linear scaling of cloud condensate amounts intended to account for subgrid-scale variability). That these two treatments agree so

TABLE 1. The impact on vertically projected cloud fraction, OLR, and reflected solar radiation at the TOA due to changes in the overlap assumption in GFDL's global model AM2. Changes are averaged over the globe and the seasonal and diurnal cycles and are relative to the default random overlap assumption. AM2 produces partially cloudy layers relatively frequently compared with other global models, so overlap assumptions can play a large role in determining the total cloud fraction and radiative fluxes.

	Exponentially decaying 1-km scale	Exponentially decaying 2-km scale	Max random	Max
Cloud fraction (%)	-4.1	-6.0	-8.6	-12.3
OLR (W m^{-2})	0.8	1.2	2.1	2.5
Reflected solar (W m^{-2})	-5.4	-7.4	-9.1	-11.9
Net radiation (W m^{-2})	4.6	6.2	7.0	9.4

TABLE 2. The impact on radiative fluxes caused by introducing subgrid-scale inhomogeneity in cloud optical thickness. The change is relative to clouds using the same overlap assumption (including the specification of length scale in the exponentially varying overlap assumption), so total cloud fraction is not affected. The variability in each grid cell is estimated from the cloud fraction and condensate amounts. Clouds in the standard model are tuned by reducing the condensate amount by 15% before radiative properties are computed; accounting for realistic amounts of inhomogeneity allows this tuning to be removed. Figures are rounded, so the total changes may differ from the sum of the components.

Relative to uniform clouds	Inhomogeneous, tuned		Inhomogeneous, untuned	
	1 km	2 km	1 km	2 km
OLR	1.3	1.4	0	0.2
Reflected solar	-3.0	-3.1	-0.5	-0.8
Net radiation (W m^{-2})	1.7	1.7	0.5	0.5

closely is no doubt lucky, but it also suggests that cloud schemes that predict (or even diagnose) the PDF of condensate may well require less arbitrary tuning than schemes that assume that clouds are homogeneous.

McICA sampling noise depends in part on the structure of the clouds in which radiative transfer is being computed, with zero bias in cloud-free columns and smaller biases when fewer layers are partially cloudy and/or if clouds are known (or assumed) to be homogeneous. Figure 3 shows the central portions of histograms of McICA sampling noise for the global cloud field produced by AM2 at a single time step. The noise is computed as the difference of McICA and full ICA calculations on the set of 25 subcolumns using the exponentially decaying overlap assumption for the rank correlation of total water with a length scale of 1 km. The standard deviation of instantaneous column-by-column sampling noise in TOA fluxes in AM2 is about 2.5 W m^{-2} for longwave radiation and 17.8 W m^{-2} for shortwave radiation—substantially smaller than estimates made from offline calculations in more complicated clouds fields (e.g., Pincus et al. 2003) even after accounting for the diurnal variation in incoming sunlight. Sampling errors in the shortwave can be much larger (up to 225 W m^{-2}) than in the longwave (up to 25 W m^{-2}) because reflected shortwave radiation depends on cloud optical thickness at all values of optical thickness, while outgoing longwave radiation (OLR) depends only on cloud-top temperature in all but the thinnest clouds (Fig. 3 does not show the largest errors). Because McICA noise is purely random, the mean error decreases as the inverse square root of the number of calculations; instantaneous global mean errors for both reflected solar and OLR are less than 0.1 W m^{-2} .

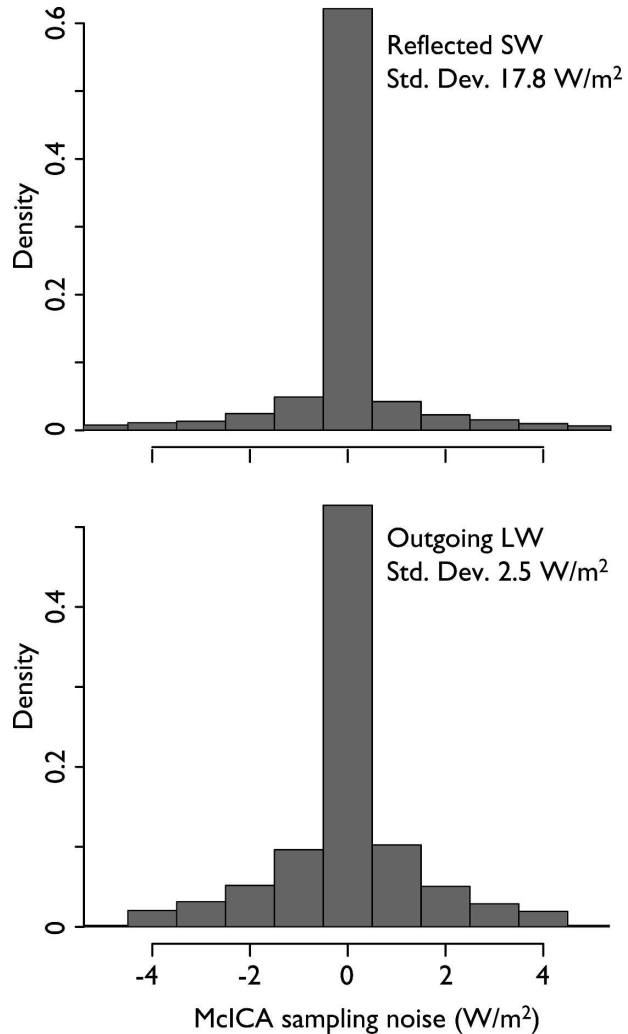


FIG. 3. Sampling noise in TOA radiative fluxes introduced by McICA in cloud fields produced by AM2. The noise is computed for a single time step using the cloud fields predicted at 0300 UTC 1 May 1983. We use an overlap assumption that changes from maximum to random exponentially with a scale length of 1 km and diagnose internal variability in cloud water and ice concentrations based on cloud fraction and mean condensate amount in each layer. McICA sampling noise is computed as the difference between McICA and ICA in each grid column. The abscissa is the same on both plots, and only the central part of both histograms is displayed. The distribution of errors in the shortwave is much broader than in the longwave, with single gridpoint errors as large as 225 W m^{-2} in the shortwave compared with 25 W m^{-2} in the longwave. Global mean errors for both sets of fluxes, though, are less than 0.1 W m^{-2} .

4. Changes in climate simulations when subcolumns are used to describe subgrid-scale cloud structure

We made three simultaneous modifications to AM2: shifting the implementation of overlap from a single

computation in each column using mean reflectance and transmittance to a set of calculations on stochastically generated subcolumns, changing the subgrid-scale assumptions from randomly overlapped homogenous clouds to inhomogeneous clouds following exponentially decaying overlap, and using McICA in lieu of a deterministic scheme (e.g., ICA) to compute the radiative fluxes. The net impact of the first two changes on radiative fluxes is fairly small in offline calculations (see section 3), so we expect a negligible impact on the model's simulated climate. The impact of the sampling noise introduced by McICA on free-running simulations, however, is less clear, because it is possible that even small amounts of sampling noise might be amplified by the many nonlinear feedbacks among clouds, radiation, and atmospheric temperature and moisture in the model. Before we can routinely incorporate our changes into AM2, we must answer two related questions. First, are climate simulations with AM2 running McICA better, worse, or about the same as those using the operational scheme? Second, are simulations with McICA different (in the sense of statistical significance) from those using the standard radiation scheme? Sampling noise from both the subcolumn generation and McICA is known to be unbiased, so different results would indicate that the sampling noise itself was processed by the model nonsymmetrically. Because sampling noise depends on the model state itself, a model that changed systematically when small random noise was introduced would be difficult to tune, as changes to the tuning would affect the mean state, which would then affect the bias produced by the sampling noise, requiring further retuning, and so on. As a point of comparison, in the National Center for Atmospheric Research (NCAR) Community Atmosphere Model (CAM), version 1.8, McICA sampling noise alone introduces statistically significant but physically unimportant changes in low cloud cover and related quantities (Räisänen et al. 2005). Because the sensitivity of any given model's simulation to sampling noise depends on both the details of the implementation (i.e., the number of subcolumns and bands used and any methods used to refine McICA, e.g., Räisänen and Barker 2004) and on the sensitivity of other parameterizations to noise in radiative fluxes, our implementation in AM2 must be tested independently of other models.

In the simulations described below, we use 25 subcolumns within each column of AM2 to represent cloud structure. Overlap changes from maximum to random inverse exponentially with a length scale of 1 km, and internal variability in cloud condensate is diagnosed from model values of grid-mean condensate and cloud fraction as described in the appendix.

a. Evaluating the climate produced by the modified global model

To assess the climate simulated by the modified model, we perform a 17-yr integration beginning 1 January 1982 using observed monthly-mean sea surface temperatures. As noted above, the model differs from the standard implementation of AM2 in three ways: it uses subcolumns to represent subgrid-scale cloud structure, incorporates new overlap assumptions, and uses McICA to compute radiative fluxes. We discard the first year of results to allow the model to "spin up."

Changes to globally averaged cloud and radiation fields between the modified and operational versions of the model are only slightly different than in the diagnostic calculations. During the last 16 yr of the 17-yr run, total cloud cover in the modified model decreases by 4.8%, with OLR increasing by 1.2 W m^{-2} and reflected shortwave radiation decreasing by 3.4 W m^{-2} . The changes to cloud cover and OLR are just slightly larger than the diagnostic calculations in which the cloud fields are held constant (see the first column of Table 1), indicating that feedbacks to the clouds and radiation fields are amplified only slightly.

Many standard diagnostics of the climate model (e.g., latitude–height plots of the zonal mean temperature or zonal wind) are nearly identical in the original and modified models. The largest changes involve the vertically projected low cloud amount, which exhibits sizable reductions over the world's oceans in the Tropics, subtropics, and at midlatitudes (Fig. 4a). Most of this change is the direct result of the change in overlap assumption, although there is a small reinforcing component from a reduction in the vertically resolved cloud amount. Vertically integrated liquid water also decreases by 10% globally (from 72 to 65 g m^{-2}), indicating that the clouds are responding slightly to the change in radiation. Changes to the reflected shortwave radiation are well correlated in space with the changes in low cloud (Fig. 4b). All changes in reflected solar radiation are accompanied by compensating changes in radiation at the surface (not shown), so there is no difference in absorption between the two runs.

Low clouds differ most strongly between the operational and modified models because the vertical resolution in both models is highest near the surface, so that near-surface layers are most strongly affected by changes in the overlap assumption. If a given (physical) layer in the atmosphere is partially cloudy, the vertically projected cloud fraction increases uniformly with the number of layers when random overlap is used but stays constant under exponentially decaying overlap. (This spurious dependence of cloud fraction on vertical

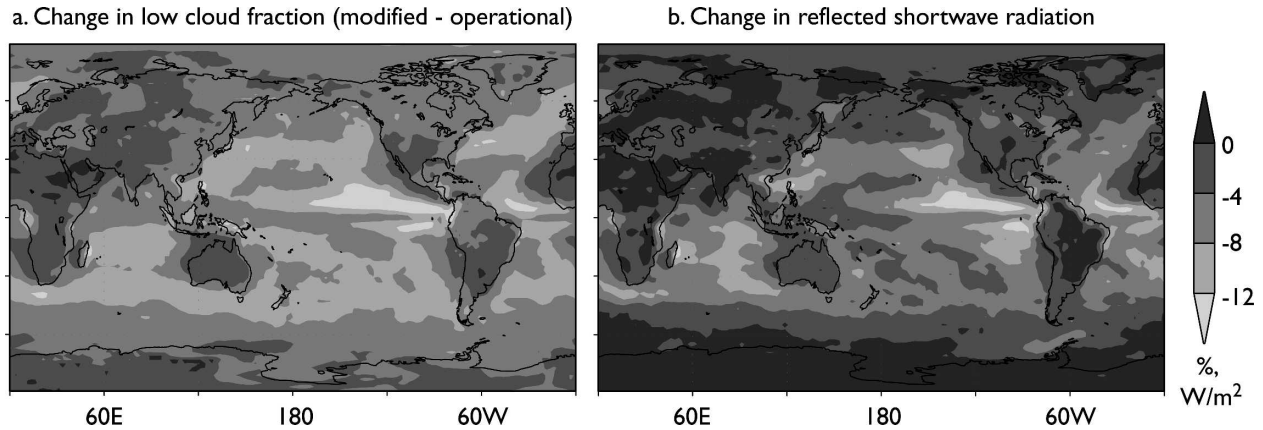


FIG. 4. The differences in (a) low cloud amount and (b) reflected shortwave radiation between the modified and operational versions of AM2. The grayscale applies to both (a) and (b), though with different units. The modified version of AM2 uses exponentially decaying overlap, diagnostic internal inhomogeneity in cloud condensate concentrations, and the McICA algorithm for computing radiative fluxes. Differences are computed over the last 16 yr of a 17-yr run with prescribed sea surface temperatures.

resolution is one of the reasons we would like to replace the random overlap assumption.) AM2 has nine levels in the lowest 1500 m of the atmosphere, while in the upper troposphere, the vertical resolution is about 2000 m. That the change in overlap determines most of the differences between the operational and modified models suggests that the implementation of stochastic sub-columns itself does not greatly affect AM2.

The effect of the overlap assumption on simulated climate is somewhat model dependent. Using the model developed by the European Centre for Medium-Range Weather Forecasts (ECMWF), for example, Morcrette and Jakob (2000) report a change in temperature in the middle and upper troposphere in excess of 1 K when the overlap assumption changed from random to maximum random. In AM2, this change is about an order of magnitude smaller, and it seems unlikely that our use of exponentially decaying overlap is the explanation. Vertical resolution, which is more uniform throughout the troposphere in the ECMWF model than in AM2, is another factor, but runs of AM2 (not shown) with substantially higher vertical resolution show only modest changes in tropospheric temperature due to our modifications.

The direct impacts of the reduction in low cloud and reflected shortwave exacerbate biases relative to standard observations of the atmosphere (GFDL Global Atmospheric Model Development Team 2004). This reflects the fact that an assumption known to contradict observations (i.e., the use of the random overlap assumption in the many shallow layers near the surface) inadvertently masked problems resulting from other parts of the model. The change in globally, annually averaged radiation between the operational and modi-

fied models is modest (2.2 W m^{-2}) but large enough to warrant a small “retuning” to bring it back into radiative balance before coupling with an ocean model. In a retuning process, some of these changes in low cloud could be counteracted.

b. Evaluating predictions of subgrid-scale variability

In addition to changing the model physics, we have added a new diagnostic, namely the parameter ϵ , which quantifies the subgrid-scale variability of cloud optical thickness. Figure 5 compares the predictions of our modified version of AM2 with the mean of this quantity as provided by ISCCP (available online at <http://isccp.giss.nasa.gov/>). The grid sizes for the two datasets are comparable near the equator, which in turn makes the estimate of ϵ comparable, because cloud variability depends on spatial scale.

Although the model shares some features with the observations, the comparison is not very encouraging. AM2 agrees with ISCCP in that tropical convective regions are more inhomogeneous than regions in which only shallow clouds are prevalent, such as the stratocumulus regions to the west of major continents, but the model greatly overestimates the amount of variability in the deep convective regions relative to observations. At higher latitudes, and over land in particular, AM2 underestimates inhomogeneity, perhaps consistent with AM2’s relatively poor representation of the subgrid variability of column cloud optical depth in frontal cloud environments (Gordon et al. 2005).

The poor agreement in Fig. 5 appears to be due to the model’s cloud optical properties (including the vertical

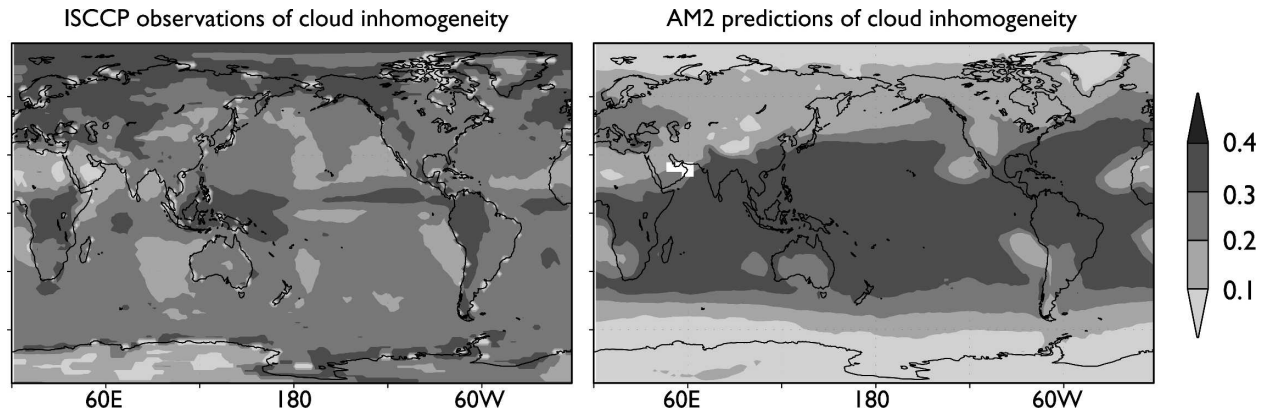


FIG. 5. Inhomogeneity factor ε , defined as one minus the ratio of the radiative-mean and linear-mean cloud optical thicknesses, as (left) observed by ISCCP and (right) predicted by the modified version of AM2. The model reproduces some basic features (e.g., the enhanced variability in the Tropics), but overall agreement is poor, mostly because of known model deficiencies in simulating the distribution of cloud optical thicknesses.

distribution of those properties) rather than to assumptions about subgrid-scale inhomogeneity (including the overlap assumption). Model predictions of subgrid-scale variability in the variability of cloud optical depth depend, in particular, only slightly on the subgrid-scale variability of cloud water content that we diagnose from the cloud fraction and mean condensate amount; ε decreases, on average, by less than 0.05 when clouds are assumed to be uniform. On the other hand, AM2 (like many global models) produces more clouds with large optical thicknesses than are observed by ISCCP (Zhang et al. 2005), and it is hard to imagine that estimates of higher-order moments of the optical depth distribution (e.g., ε , which is roughly related to both the mean and the variance of cloud optical depth) would agree with observations when the agreement of the mean is poor.

c. Do simulations made using McICA differ from those using more accurate radiation calculations?

The climate simulated by AM2 in its new configuration does not differ in dramatic ways from the default configuration, but there remains the question as to whether sampling noise can cause discernible systematic shifts in the model's climate. To answer this question, we must compare any systematic changes that occur when McICA is used to the internal variability of the model in both its approximate (McICA) and deterministic (ICA) modes. To this end, we construct two 10-member ensembles by selecting the state of the simulation described in the previous section on the first 10 days of model year 1990 as initial conditions for a 1-yr integration. The simulations are identical except that, in one ensemble, a full broadband radiation calcu-

lation is performed on each of the 25 subcolumns in each model column (i.e., the ICA is used), while the other ensemble uses McICA.

The variability in cloud and radiation-related fields within each of these ensembles is substantially larger than the mean difference between them. The top two panels of Fig. 6 show the variability in annually averaged reflected shortwave radiation within the ICA and McICA ensembles, respectively, computed as the set of differences between the ensemble mean and the value at each grid point in each ensemble member. (Histograms for the operational version of AM2, not shown, are indistinguishable from the ICA and McICA ensembles.) The lowest panel shows the gridpoint differences between the ensemble-mean ICA and McICA calculations, which has a much narrower distribution than is obtained within either ensemble. As a quantitative test of statistical significance, we use a Student's t test applied at each grid point. The null hypothesis for this test is that the mean of the two samples being tested (in this case, 10 pairs of a given cloud or radiation quantity at a given location) is the same; the significance level (p value) for the test indicates the likelihood that the means of two samples drawn from a single distribution might be expected to differ by a given amount by chance alone. Figure 7 shows the significance levels for annually averaged reflected solar radiation. These values are distributed approximately uniformly between 0 and 1, consistent with the hypothesis that the ICA and McICA runs are statistically indistinguishable. These results are similar to those for longwave and shortwave radiation fields at the surface and TOA, as well as low, middle, and high cloud amounts.

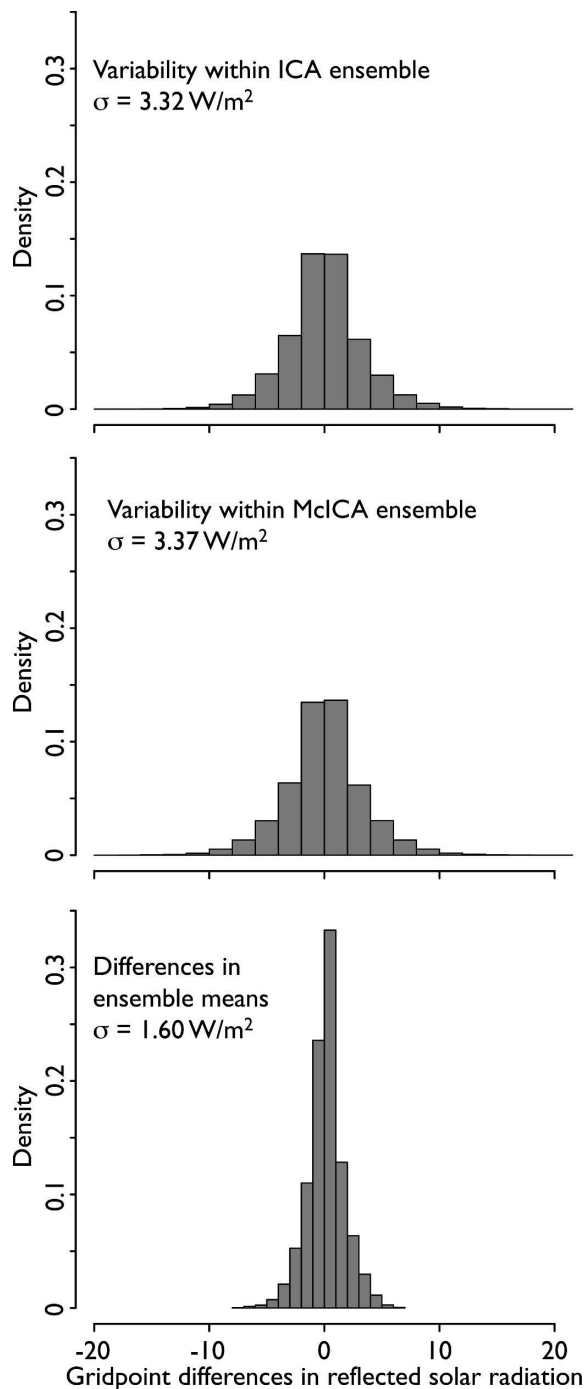


FIG. 6. Distribution of differences of mean annually averaged reflected shortwave radiation within and between two ensembles of year-long simulations. (top) The distribution of gridpoint differences of each ensemble member from the ensemble mean when a complete radiation calculation is performed in each subcolumn (ICA), (middle) same result for the ensemble using McICA, and (bottom) the distribution of differences between the two ensemble means at each grid point. There is substantially more variability within the ensembles than between them, indicating that the use of McICA does not change the climate simulated by AM2.

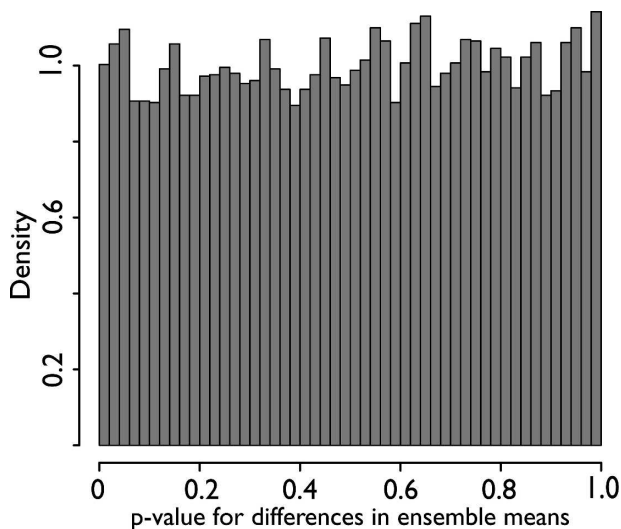


FIG. 7. Significance values (p values) for a Student's t test applied to the difference in ensemble-mean annually averaged reflected solar radiation at each grid point between ensembles of simulations using ICA and McICA. This value indicates the likelihood that the means of two samples drawn from a single distribution would be expected to differ by a given amount by chance alone. The uniform distribution of these values confirms that the ICA and McICA simulations are statistically indistinguishable.

5. Conclusions

We have described changes to the way subgrid-scale cloud structure is represented in AM2, and have used the new technique's flexibility to implement new assumptions regarding horizontal and vertical variability. As it turns out, the net effect of these impacts on radiative fluxes is small because the changes caused by the new overlap assumption act, by chance, to oppose the change incurred when the operational implementation is replaced with subcolumns. The new schemes have not produced immediate improvements in the climate simulated by AM2 but the model is now completely flexible with respect to assumptions about subgrid-scale structure in clouds (and potentially water vapor). The diagnostic variability in cloud condensate used here may be replaced with a distribution drawn from an assumed-PDF cloud scheme (Tompkins 2002), for example, with no further modifications, and the radiative effects of convective clouds [e.g., those treated by the Donner (1993) convection scheme under development at GFDL] included in a consistent way. One might also simply specify relationships between cloud horizontal variability, vertical structure, and cloud amount and concentration (e.g., Räisänen et al. 2004) based on observations, although this is more attractive in models without an internal representation of small-scale variability.

Subcolumns might be used to account for the effects of subgrid-scale variability on other processes. Cloud microphysical processes, for example, could be computed in each subcolumn (Jakob and Klein 2000) to account for both arbitrary overlap assumptions and arbitrary distributions of condensate amount in each level, though this will be prohibitively time-consuming until methods for speeding up the calculation can be developed. Subcolumns could also be used to represent the subgrid-scale variability of water vapor, particularly when using assumed-PDF schemes in which this distribution is explicitly available; variable relative humidity might then be used to help predict aerosol size distributions for clear-sky radiation calculations or used in lieu of the mean sounding to link convection to the large-scale environment.

The process of replacing profiles of continuously variable cloud properties with finite sets of discrete, locally uniform subcolumns introduces sampling noise, and the use of the McICA to compute radiative transfer adds another layer of noise. We demonstrated in section 4 that McICA noise does not systematically affect the evolution of clouds and radiation in AM2 as it does the NCAR Community Atmosphere Model. This is likely related to the very different ways the two models determine cloud fraction, because the NCAR model's diagnostic cloud fraction scheme is more easily affected by instantaneous anomalies in local heating and cooling rates than the prognostic scheme used by AM2. The initial discretization of model columns also introduces sampling noise, but this is relatively small (e.g., an RMSE of 10% or less in cloud fraction when 25 columns are used), especially compared with the accuracy of the underlying cloud scheme. In neither CAM nor AM2 does the climate degrade when sampling noise is introduced, consistent with the results from short-term forecasts (Pincus et al. 2003). This suggests that global models are forgiving enough to admit radiation parameterizations that are unbiased but approximate.

Acknowledgments. This research was supported by the Office of Science (BER), U.S. Department of Energy (Grant DE-FG02-03ER63561), and by the National Science Foundation (Grant ATM-0336702) as part of the Climate Processes Team on Low-Latitude Cloud Feedbacks on Climate Sensitivity. The Geophysical Fluid Dynamics Laboratory supported an extended visit by R. Pincus. The contribution of S. A. Klein was performed under the auspices of the U.S. Department of Energy at the University of California Lawrence Livermore National Laboratory under Contract W-7405-Eng-48. We appreciate the comments of

Xianglei Huang, Isaac Held, and two anonymous reviewers.

APPENDIX

Diagnosing Subgrid-Scale Inhomogeneity in Cloud Condensate

AM2 predicts three cloud properties—cloud area fraction q_a , cloud liquid water specific humidity q_l , and cloud ice specific humidity q_i —within each grid cell. We are considering replacing this parameterization with one that predicts the distribution of total water mixing ratio $q_t = q_v + q_l + q_i$ (where q_v is the water vapor specific humidity), from which the PDF of cloud liquid and ice can be inferred (Tompkins 2002). Here, we describe a method for diagnosing a PDF of total water that is consistent both with the current cloud scheme (i.e., the values of cloud fraction and condensate $q_c = q_l + q_i$ predicted in AM2) and the scheme under development (i.e., the distribution of total water). This placeholder allows us to get a rough idea of how much subgrid-scale variability might affect radiation and precipitation fluxes before devoting the considerable time and effort needed to build a full assumed-PDF cloud scheme.

The PDF scheme assumes that the total water specific humidity within each model grid cell follows a beta distribution. This distribution is specified by four parameters: the exponents p and q (which determine the shape of the distribution) and the minimum and maximum values a and b . The cloud fraction and grid-mean condensate amounts are then given by Tompkins (2002) as

$$q_a = 1 - I_{\tilde{q}_s}(p, q) \quad \text{and} \quad (A1)$$

$$q_c = \alpha \left\{ (b - a) \frac{p}{p + q} [1 - I_{\tilde{q}_s}(p + 1, q)] - (q_s - a) q_a \right\}, \quad (A2)$$

where we use the incomplete gamma function $I_x(p, q)$ and the normalized saturation (equilibrium) specific humidity

$$\tilde{q}_s = \frac{q_s - a}{b - a}. \quad (A3)$$

Equation (A2) differs from (14) in Tompkins (2002) in that we have included the thermodynamic factor

$$\alpha = 1 \left/ \left(1 + \frac{L}{c_p} \frac{\partial q_s}{\partial T} \Big|_{T_f} \right) \right., \quad (A4)$$

where T_f is the “frozen temperature,” including the latent heats of vaporization and sublimation

$T_f = T - L_v q_l - L_s q_i$. This is equivalent to assuming that energy is constant within the grid cell, while Tompkins assumes constant temperature; this choice does not strongly affect the distribution we obtain because the total condensate in (A2) is predicted by a separate scheme.

The beta distribution is described by four parameters, but we have, at most, two pieces of information (cloud fraction and mean condensate concentration). To completely determine the distribution, we specify q and assume $p = q$ (i.e., that the distribution of total water is symmetric). We use a lookup table of incomplete beta distribution deviates to find the value of \tilde{q}_s that solves (A1), then solve (A2) for the distribution width $b - a$. When cloud fraction is unity, we assume that the minimum value of q_i in the grid cell is just saturated; because the distribution is assumed symmetric, this is equivalent to specifying $b - a = 2q_c/\alpha$. Note that the distribution of condensate (as opposed to total water) is symmetric only when the cloud fraction is 1 and is quite skewed toward small values when the cloud fraction is less than 0.5.

To create sample i from the distribution, we choose a random number from a uniform distribution between zero and one, then use the beta distribution deviate table to determine the scaled value of total water $\tilde{q}_{t,i} = (q_{t,i} - a)/(b - a)$, from which we determine the condensate specific humidity in those subcolumns containing cloud as $q_{c,i} = \alpha(b - a)(\tilde{q}_{t,i} - \tilde{q}_s)$. This condensate is then partitioned into ice and liquid in each subcolumn according to the ratio from the global model grid cell.

The distribution we determine through this procedure also implies a mean vapor specific humidity that may differ from the value predicted by AM2. Constraining the PDF to simultaneously have the same mean vapor, cloud fraction, and cloud condensate as the model adds considerable complication to the diagnostic calculation. As vapor is not used in our calculations, allowing the vapor to be inconsistent with the PDF seems acceptable.

REFERENCES

- Barker, H. W., and Coauthors, 2003: Assessing 1D atmospheric solar radiative transfer models: Interpretation and handling of unresolved clouds. *J. Climate*, **16**, 2676–2699.
- Bergman, J. W., and P. J. Rasch, 2002: Parameterizing vertically coherent cloud distributions. *J. Atmos. Sci.*, **59**, 2165–2182.
- Donner, L. J., 1993: A cumulus parameterization including mass fluxes, vertical momentum dynamics, and mesoscale effects. *J. Atmos. Sci.*, **50**, 889–906.
- GFDL Global Atmospheric Model Development Team, 2004: The new GFDL global atmosphere and land model AM2–LM2: Evaluation with prescribed SST simulations. *J. Climate*, **17**, 4641–4673.
- Gordon, N. D., J. R. Norris, C. P. Weaver, and S. A. Klein, 2005: Cluster analysis of cloud regimes and characteristic dynamics of midlatitude synoptic systems in observations and a model. *J. Geophys. Res.*, **110**, D15S17, doi:10.1029/2004JD005027.
- Hogan, R. J., and A. J. Illingworth, 2000: Deriving cloud overlap statistics from radar. *Quart. J. Roy. Meteor. Soc.*, **126**, 2903–2909.
- , and —, 2003: Parameterizing ice cloud inhomogeneity and the overlap of inhomogeneities using cloud radar data. *J. Atmos. Sci.*, **60**, 756–767.
- Jakob, C., and S. A. Klein, 2000: A parametrization of the effects of cloud and precipitation overlap for use in general-circulation models. *Quart. J. Roy. Meteor. Soc.*, **126**, 2525–2544.
- Klein, S. A., and C. Jakob, 1999: Validation and sensitivities of frontal clouds simulated by the ECMWF model. *Mon. Wea. Rev.*, **127**, 2514–2531.
- Larson, V. E., J.-C. Golaz, H. Jiang, and W. R. Cotton, 2005: Supplying local microphysics parameterizations with information about subgrid variability: Latin hypercube sampling. *J. Atmos. Sci.*, **62**, 4010–4026.
- Mace, G. G., and S. Benson-Troth, 2002: Cloud-layer overlap characteristics derived from long-term cloud radar data. *J. Climate*, **15**, 2505–2515.
- Matsumoto, M., and T. Nishimura, 1998: Mersenne twister: A 623-dimensionally equidistributed uniform pseudo-random number generator. *ACM Trans. Model. Comput. Simul.*, **8**, 3–30.
- Mlawer, E. J., S. J. Taubman, P. D. Brown, M. J. Iacono, and S. A. Clough, 1997: Radiative transfer for inhomogeneous atmospheres: RRTM, a validated correlated- k model for the longwave. *J. Geophys. Res.*, **102D**, 16 663–16 682.
- Morcrette, J. J., and C. Jakob, 2000: The response of the ECMWF model to changes in the cloud overlap assumption. *Mon. Wea. Rev.*, **128**, 1707–1732.
- Pincus, R., H. W. Barker, and J. J. Morcrette, 2003: A fast, flexible, approximate technique for computing radiative transfer in inhomogeneous cloud fields. *J. Geophys. Res.*, **108**, 4376, doi:10.1029/2002JD003322.
- , C. Hannay, S. A. Klein, K.-M. Xu, and R. S. Hemler, 2005: Overlap assumptions for assumed probability distribution function cloud schemes in large scale models. *J. Geophys. Res.*, **110**, D15S09, doi:10.1029/2004JD005100.
- Press, W. H., B. P. Flannery, S. A. Teukolsky, and W. T. Vetterling, 1986: *Numerical Recipes: The Art of Scientific Computing*. Cambridge University Press, 818 pp.
- Räisänen, P., and H. W. Barker, 2004: Evaluation and optimization of sampling errors for the Monte Carlo Independent Column Approximation. *Quart. J. Roy. Meteor. Soc.*, **130**, 2069–2085.
- , —, M. F. Khairoutdinov, J. Li, and D. A. Randall, 2004: Stochastic generation of subgrid-scale cloudy columns for large-scale models. *Quart. J. Roy. Meteor. Soc.*, **130**, 2047–2067.
- , —, and J. N. S. Cole, 2005: The Monte Carlo Independent Column Approximation's conditional random noise: Impact on simulated climate. *J. Climate*, **18**, 4715–4730.
- Rossow, W. B., and R. A. Schiffer, 1999: Advances in understanding clouds from ISCCP. *Bull. Amer. Meteor. Soc.*, **80**, 2261–2287.
- , C. Delo, and B. Cairns, 2002: Implications of the observed mesoscale variations of clouds for the Earth's radiation budget. *J. Climate*, **15**, 557–585.

- Tian, L., and J. A. Curry, 1989: Cloud overlap statistics. *J. Geophys. Res.*, **94D**, 9925–9935.
- Tiedtke, M., 1996: An extension of cloud-radiation parameterization in the ECMWF model: The representation of subgrid-scale variations of optical depth. *Mon. Wea. Rev.*, **124**, 745–750.
- Tompkins, A. M., 2002: A prognostic parameterization for the subgrid-scale variability of water vapor and clouds in large-scale models and its use to diagnose cloud cover. *J. Atmos. Sci.*, **59**, 1917–1942.
- Webb, M., C. Senior, S. Bony, and J. J. Morcrette, 2001: Combining ERBE and ISCCP data to assess clouds in the Hadley Centre, ECMWF and LMD atmospheric climate models. *Climate Dyn.*, **17**, 905–922.
- Yu, W., M. Doutriaux, G. Seze, H. LeTreut, and M. Desbois, 1996: A methodology study of the validation of clouds in GCMs using ISCCP Satellite observations. *Climate Dyn.*, **12**, 389–401.
- Zhang, M. H., and Coauthors, 2005: Comparing clouds and their seasonal variations in 10 atmospheric general circulation models with satellite measurements. *J. Geophys. Res.*, **110**, D15S02, doi:10.0129/2004JD005021.